THE JOURNAL OF BIOLOGICAL CHEMISTRY Vol. 277, No. 37, Issue of September 13, pp. 34336–34342, 2002
Printed in U.S.A.

Structures of the Complexes of a Potent Anti-HIV Protein Cyanovirin-N and High Mannose Oligosaccharides*

Received for publication, June 13, 2002, and in revised form, July 8, 2002
Published, JBC Papers in Press, July 10, 2002, DOI 10.1074/jbc.M205909200

Istvan Botos‡, Barry R. O'Keefe§, Shilpa R. Shenoy§, Laura K. Cartner¶, Daniel M. Ratner‖, Peter H. Seeberger‖‡‡, Michael R. Boyd§§, and Alexander Wlodawer‡¶¶**

From the ‡Macromolecular Crystallography Laboratory, NCI, National Institutes of Health, Frederick, Maryland 21702-1201, §Molecular Targets Drug Discovery Program, Center for Cancer Research, NCI–Frederick, National Institutes of Health, Frederick, Maryland 21702, ¶Intramural Research Support Program, SAIC-Frederick, Frederick, Maryland 21702, ‖Department of Chemistry, Massachusetts Institute of Technology, Cambridge, Massachusetts 02139, and the §§USA Cancer Research Institute, College of Medicine, University of South Alabama, Mobile, Alabama 36688

The development of anti-human immunodeficiency virus (HIV) microbicides for either topical or *ex vivo* use is of considerable interest, mainly due to the difficulties in creating a vaccine that would be active against multiple clades of HIV. Cyanovirin-N (CV-N), an 11-kDa protein from the cyanobacterium (blue-green algae) *Nostoc ellipsosporum* with potent virucidal activity, was identified in the search for such antiviral agents. The binding of CV-N to the heavily glycosylated HIV envelope protein gp120 is carbohydrate-dependent. Since previous CV-N-dimannose structures could not fully explain CV-N-oligomannose binding, we determined the crystal structures of recombinant CV-N complexed to Man-9 and a synthetic hexamannoside, at 2.5- and 2.4-Å resolution, respectively. CV-N is a three-dimensional domain-swapped dimer in the crystal structures with two primary sites near the hinge region and two secondary sites on the opposite ends of the dimer. The binding interface is constituted of three stacked α1→2-linked mannose rings for Man-9 and two stacked mannose rings for hexamannoside with the rest of the saccharide molecules pointing to the solution. These structures show unequivocally the binding geometry of high mannose sugars to CV-N, permitting a better understanding of carbohydrate binding to this potential new lead for the design of drugs against AIDS.

Of the more than 30 million people infected with HIV[1] before 1997, 75–85% acquired the virus through heterosexual contacts (1); thus AIDS is likely to continue to affect the general population. The development of a vaccine active against multiple clades of HIV is complicated by the high mutation rate of the virus (2). In the absence of vaccines, there is a growing interest in the development of anti-HIV virucides for either topical or *ex vivo* use (3). A unique natural product identified in the search for new antiviral agents was cyanovirin-N (CV-N), originally isolated from cultures of the cyanobacterium (blue-green algae) *Nostoc ellipsosporum* (4).

Nanomolar concentrations of CV-N potently inactivate diverse strains of HIV-1, HIV-2, SIV, and FIV (4, 5), acting at the level of the virus, not the target cell, to abort the infection process. This is achieved by preventing essential interactions between the envelope glycoprotein and target cell receptors (4–6). For HIV-1, glycoprotein gp120 is primarily involved in cell entry with approximately half of its molecular weight provided by carbohydrates (7). Out of the 24 *N*-linked oligosaccharides found on its surface, 11 are high mannose or hybrid type (8). Studies have shown that the binding of CV-N to gp120 is carbohydrate-dependent (4, 6, 9). Moreover, CV-N also binds free *N*-linked oligosaccharides, having nanomolar affinity for the D1D3 isomer of Man-8 and oligomannose-9 (Man-9) (10–12) and directly competing with gp120 for CV-N binding. NMR and isothermal titration calorimetry experiments have shown that the binding sites exhibit different affinities for the high mannose oligosaccharides (13).

CV-N, a 101-amino acid protein, exists in solution as either a compact monomer or a dimer, whereas all crystal structures show it exclusively as three-dimensional domain-swapped dimers (14–19). Three-dimensional domain swapping is an oligomerization process in which two or more protein chains exchange identical domains (20).

Monomeric CV-N consists of two similar domains with an overall ellipsoidal shape. Although the sequence of the protein is duplicated with over 60% identity between residues 1–50 and 51–101, domain definitions based on the primary and tertiary structures do not coincide exactly. Sequence-defined domain A consists of residues 1–50, whereas residues 51–101 form domain B. Each domain contains mostly β-strands and loops. Two intramolecular disulfide bonds (C8-C22, C58-C73) are important for the structural stability and anti-HIV activity (21). A change of torsion angles in the hinge region (residues 49–54) separates domains A and B of CV-N into an extended form in

* This work was supported in part by federal funds from the NCI, National Institutes of Health under Contract Number N01-CO-12400. The costs of publication of this article were defrayed in part by the payment of page charges. This article must therefore be hereby marked "*advertisement*" in accordance with 18 U.S.C. Section 1734 solely to indicate this fact.

The atomic coordinates and structure factors (code 1M5J, 1M5M) have been deposited in the Protein Data Bank, Research Collaboratory for Structural Bioinformatics, Rutgers University, New Brunswick, NJ (http://www.rcsb.org/).

** Supported financially by the National Institutes of Health Biotechnology Training Grant.

‡‡ A GlaxoSmithKline Research Scholar and an Alfred P. Sloan Scholar.

¶¶ To whom correspondence should be addressed: NCI, National Institutes of Health, MCL Bldg. 536, Rm. 5, Frederick, MD 21702-1201. Tel.: 301-846-5036; Fax: 301-846-6128; E-mail: wlodawer@ncifcrf.gov.

[1] The abbreviations used are: HIV, SIV, and FIV are human, simian, and feline immunodeficiency viruses, respectively; CV-N, cyanovirin-N; gp120, 120-kDa surface envelope glycoprotein of HIV; gp41, 41-kDa transmembrane subunit of HIV envelope; ITC, isothermal titration calorimetry; CHES, 2-(cyclohexylamino)ethanesulfonic acid; CAPS, 3-(cyclohexylamino)-1-propanesulfonic acid; CAPSO, 3-(cyclohexylamino)-2-hydroxypropanesulfonic acid.

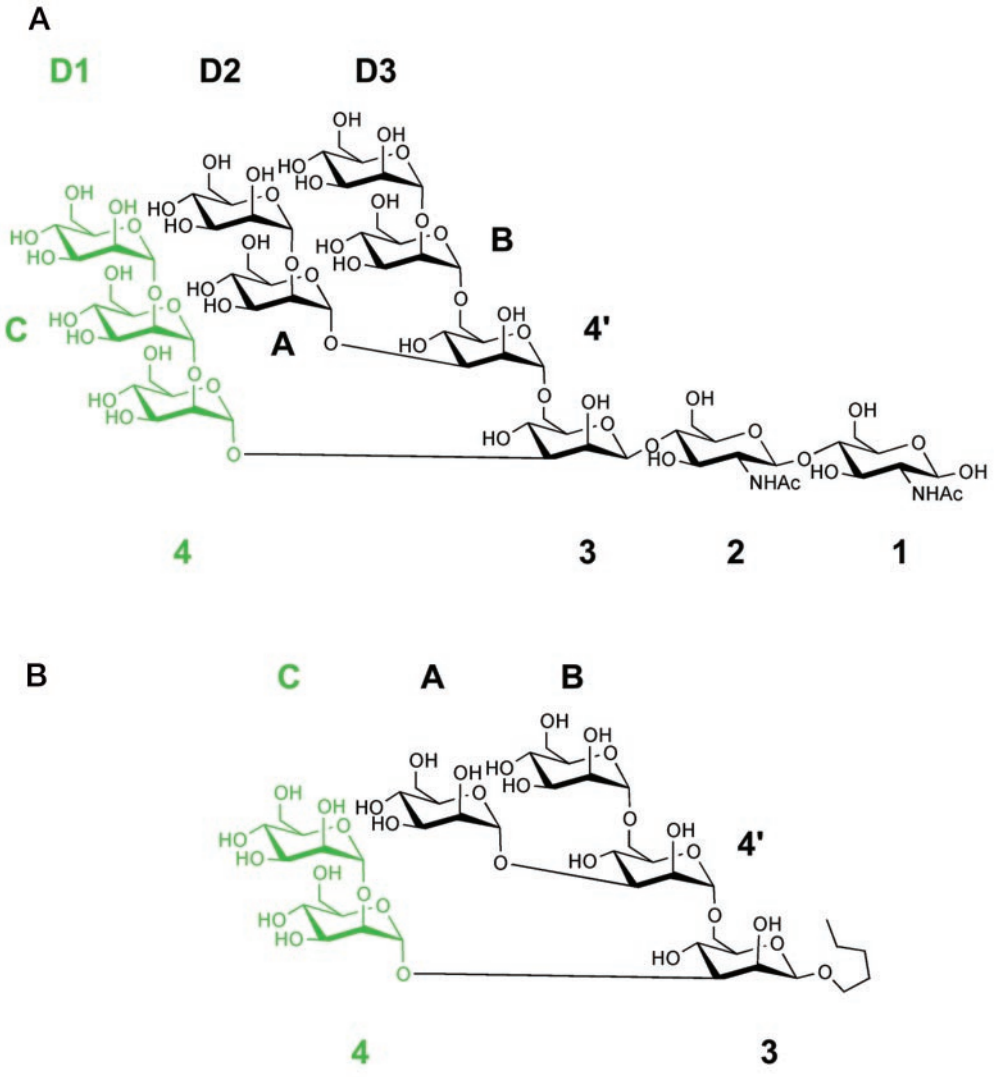

FIG. 1. **Chemical structures of oligosaccharides.** Man-9 (*A*) and synthetic hexamannoside (*B*), used in these studies, are displayed with standard *numbering* and the binding interface highlighted in *green*.

which they do not contact each other. A domain-swapped dimer is formed by two such symmetrically related extended monomers in which domain A comes in contact with domain B′ from a different chain, the overall structure of each pseudo-monomer (AB′ and A′B) being virtually identical to the compact monomer with the exception of the hinge residues. Although the structures of individual pseudo-monomers resemble the compact monomer very closely, the relative orientation of the pseudo-monomers vary widely between different structures (19, 22). Crystal packing seems to thermodynamically favor the dimeric form, selectively trapping this form in the growing crystals, decreasing the abundance of the dimer in solution, and shifting the equilibrium from monomer to dimer.

Since the antiviral activity of CV-N results from its binding to carbohydrates, understanding the structural basis of such interactions is important for the potential development of this protein as an anti-AIDS agent. In the present study, we report medium resolution structures of the complexes of wild-type CV-N with the oligosaccharide Man-9 (Fig. 1*A*) and with a synthetic hexamannoside (Fig. 1*B*).

EXPERIMENTAL PROCEDURES

High Mannose Saccharides—Man-9 was purchased from Glyko Inc. (Novato, CA). Solution phase synthesis of the branched hexamannoside has been described previously (23).

Isothermal Titration Calorimetry Experiments—The calorimetric titrations were performed on a VP™-isothermal titration calorimetry (ITC) titration calorimeter from Microcal, Inc. (Northampton, MA). In a typical experiment, 10-μl aliquots of a CHES solution were injected from a 250-μl syringe into a rapidly mixing (300 rpm) solution of CV-N (cell volume, 1.3472 ml). Control experiments involved injecting identical amounts of the CHES solution into buffer without CV-N. The concentration of CV-N was 0.463 mM, and that of CHES was 6.48 mM. Titrations were carried out at 30 °C in 50 mM sodium phosphate buffer, 0.2 M NaCl, 0.02% NaN_3, pH 7.5. The isotherms, corrected for dilution/buffer effects, were fit using the Origin ITC Analysis software according to the manufacturer's protocols. A nonlinear least square method was used to fit the titration data and to calculate the errors. From the binding curve values for enthalpy, stoichiometry, and binding affinity were extracted. Thermodynamic parameters were calculated using $\Delta G = -RT\ln K_a$, $\Delta G = \Delta H - T\Delta S$.

Protein Purification and Crystallization—Wild-type CV-N was cloned, expressed, and purified from *Escherichia coli* as reported previously (24). Only crystals grown at high pH in silica hydrogel (Hampton Research) were successfully utilized for preparation of complexes with oligosaccharides. These crystals were grown from droplets containing an equal mixture of protein and precipitant (1 M sodium citrate and 0.1 M CHES, pH 10.3). After 14 days at room temperature, the crystals grew to 0.2 × 0.15 × 0.1 mm. Crystals were soaked for 48 h in 1 mM Man-9 or hexamannose immediately before data collection. CV-N-hexamannose co-crystals grew under a range of conditions under which the wild-type CV-N alone would not crystallize.

Crystallographic Procedures—X-ray data for the CV-N-oligosaccha-

TABLE I
Crystallographic statistics

	Man-9	Hexamannoside
Diffraction data statistics		
Cell parameters	a = b = 61.51, c = 147.94 $\alpha = \beta = \gamma = 90.0$	a = b = 61.35, c = 147.56 $\alpha = \beta = \gamma = 90.0$
Space group	$P4_12_12$	$P4_12_12$
Molec/asymmetric unit	1	1
Resolution (Å)	2.5	2.4
Total reflections	214,251	129,116
Unique reflections	7,967	11,728
Completeness (%)	99.9	99.8
Last shell	100.0	99.6
Avg. I/σ	23.0	12.1
R_{merge} (%)[a]	7.1	5.6
Refinement statistics		
R-factor (%)[b]	24.2	22.4
R_{free} (%)[c]	29.8	28.9
R.m.s.d. bonds (Å)[d]	0.009	0.01
Angles (deg)	1.6	1.8

[a] $R_{merge} = \Sigma|I - \langle I\rangle|/\Sigma I$, where I is the observed intensity, and $\langle I\rangle$ is the average intensity obtained from multiple observations of symmetry-related reflections after rejections.
[b] R-factor = $\Sigma||F_o| - |F_c||/\Sigma|F_o|$, where F_o and F_c are the observed and calculated structure factors, respectively.
[c] R_{free} defined in Ref. 38.
[d] R.m.s.d., root mean square deviation.

ride complexes were collected at 100 K on beamline X9B, National Synchrotron Light Source (NSLS), Brookhaven National Laboratory, with the ADSC Quantum4 CCD detector, at 0.92-Å wavelength. A cryoprotectant, consisting of 80% mother liquor and 20% ethylene glycol, was used. Data were processed with HKL2000 (25) (Table I). Molecular replacement was carried out with AmoRe (26) using a compact monomer as a search model. With the correct solution, the symmetry-related mates were generated, and although domain A was kept fixed, domain B was superimposed over the closest symmetry mate in the linker region. The molecular replacement could not be carried out with the extended molecule (Protein Data Bank code 3ezm) due to the relative reorientation of the two domains under different conditions. The CNS (27) maximum likelihood refinement procedure was used, combined with simulated annealing. The model was rebuilt into density using O (28) with the oligosaccharide models generated with InsightII (Accelrys) and parameterized using XPLO-2D (29).

RESULTS AND DISCUSSION

The Overall Structure of CV-N—Two different crystal forms of CV-N have been described. Trigonal crystals grow predominantly at low pH (4.6) (15), whereas tetragonal crystals grow at high pH (9.5–10.3) (19). The structures of the pseudo-monomers of CV-N seen in both crystal forms are very similar (Fig. 2A), but their relative orientation is quite different (19), and the intermolecular contacts are distinct. Only the tetragonal crystals could be used successfully for the determination of the structures of oligosaccharide complexes.

Oligosaccharides and Their Binding—Two branched high mannose oligosaccharides were used in this study. Man-9 was derived from natural sources, and its structure corresponds to an oligosaccharide that is part of the HIV-1 envelope glycoprotein gp120. The structure (Fig. 1*A*) is made up of a reducing end consisting of two β1→4-linked *N*-acetyl glucosamine residues that form a chitobiose unit followed by 9 mannose residues that form a branching, triantennary structure. The second oligosaccharide (Fig. 1*B*) is a synthetic structure with six mannoses linked similarly to the core structure of Man-9, excluding the chitobiose unit on the reducing end (replaced by a pentyl group) and the terminal mannose units from the triantennary arms of Man-9.

CV-N has been reported to bind to Man-9 with nanomolar (13–20 nM) affinity (10, 13) and to a synthetic hexamannoside with low micromolar (2.6 μM) affinity (13). There are two distinct sugar-binding sites in a CV-N monomer, located ~35 Å away from each other: a high affinity primary site and a low affinity secondary site (10). These sites were mapped to the surface of CV-N by NMR perturbation studies even before any direct structural data on oligosaccharide binding became available. Residues 41–44, 50–56, and 74–78 define the primary site, whereas residues 1–7, 22–26, and 92–95 form the secondary site (10). In a domain-swapped dimer, there are four sugar-binding sites: two primary sites near the hinge region and two secondary sites on the opposite sides of the dimer, where it is not influenced by the conformation of the hinge region. In the domain-swapped dimer, the sugar-binding sites are formed by intertwined loops of residues belonging to both monomers. For example, the secondary site is created by residues 1–7 and 22–26 from the first monomer and residues 92′-95′ and 101′ from the second monomer.

The primary sugar-binding site consists of a deep pocket in the close proximity of the hinge region, which can accommodate an α1→2-linked dimannose molecule (30) (Fig. 2*B*). In our structures (Table I), there was no sugar bound in the primary site over a wide pH range, regardless of crystal soaking or co-crystallization with the oligosaccharide. Instead, there was a well defined, tightly bound CHES molecule from the crystallization solution, partially obstructing the pocket and forming a strong hydrogen bond anchoring the sulfate oxygen atom O13 to Arg-76 NH_2 of CV-N. Further interactions with CV-N were mainly hydrophobic, through the cyclohexyl ring of CHES. The buffer molecule did not bind the secondary sugar-binding site, even in the absence of any sugar. As crystals can be grown in other buffers in the same pH range (CAPS, CAPSO, AMP, glycine, and ethanolamine), it was unlikely that the CHES molecule was involved in any critical packing interactions. We assessed the binding affinity of CHES to CV-N using the technique of ITC (Table II). We have used ITC previously to characterize the binding interactions of various oligomannoses to CV-N (13). The binding interaction between CHES and CV-N was very weak (K_d value of ~0.1–0.5 mM) and characterized by few polar/electrostatic interactions (ΔH value of ~0.2 kcal/mol). This was unlike the oligomannose-CV-N interactions in which strong favorable binding enthalpies (ΔH value of ~−20 kcal/mol) had resulted in submicromolar CV-N binding affinities (K_d 0.02–50 μM) for the oligomannoses (13). Given these calorimetric data, it is highly unlikely that CHES could have prevented oligosaccharide binding.

Comparison of crystal (15, 19) and solution (14, 30) structures of CV-N reveals the changing geometry of the primary

sugar-binding site upon domain swapping (Fig. 3). We can only speculate on the significance, if any, of this shift in the relative orientation of the two domains. Since the primary sugar-binding site is in close proximity to the hinge region, the position of the hinge and relative orientation of the domains has a direct impact on the shape of the primary sugar-binding site. In the monomer, the pocket is intact, accommodating a disaccharide in a stacked conformation (30), whereas in all domain-swapped structures, some of the essential protein-oligosaccharide hydrogen bonds cannot be established, leaving only the shape

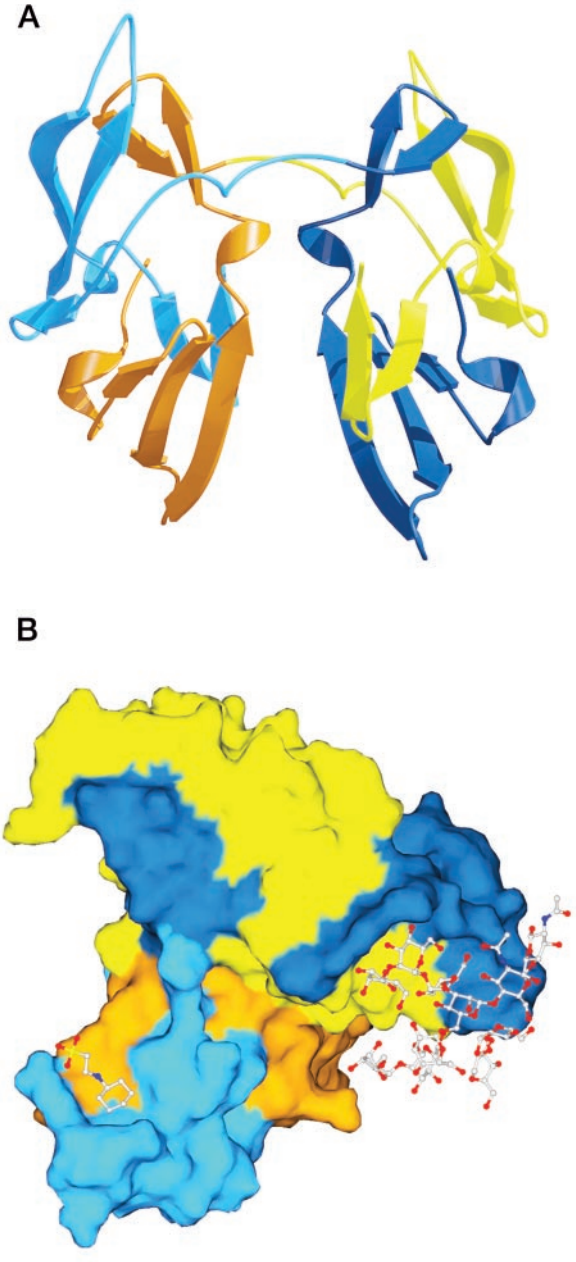

FIG. 2. **The domain-swapped CV-N dimer.** *A*, dimer with the sequence-defined domains A (*dark blue*) and B (*light blue*) from the first molecule and domains A′ (*orange*) and B′ (*yellow*) from the second molecule. AB′ and A′B are pseudo-monomers. Molecular surface (*B*) with the primary and secondary oligosaccharide-binding sites with CHES bound to the former and Man-9 to the latter. Both parts of this figure were generated with programs Bobscript (39), Raster3D (40), and SPOCK (41).

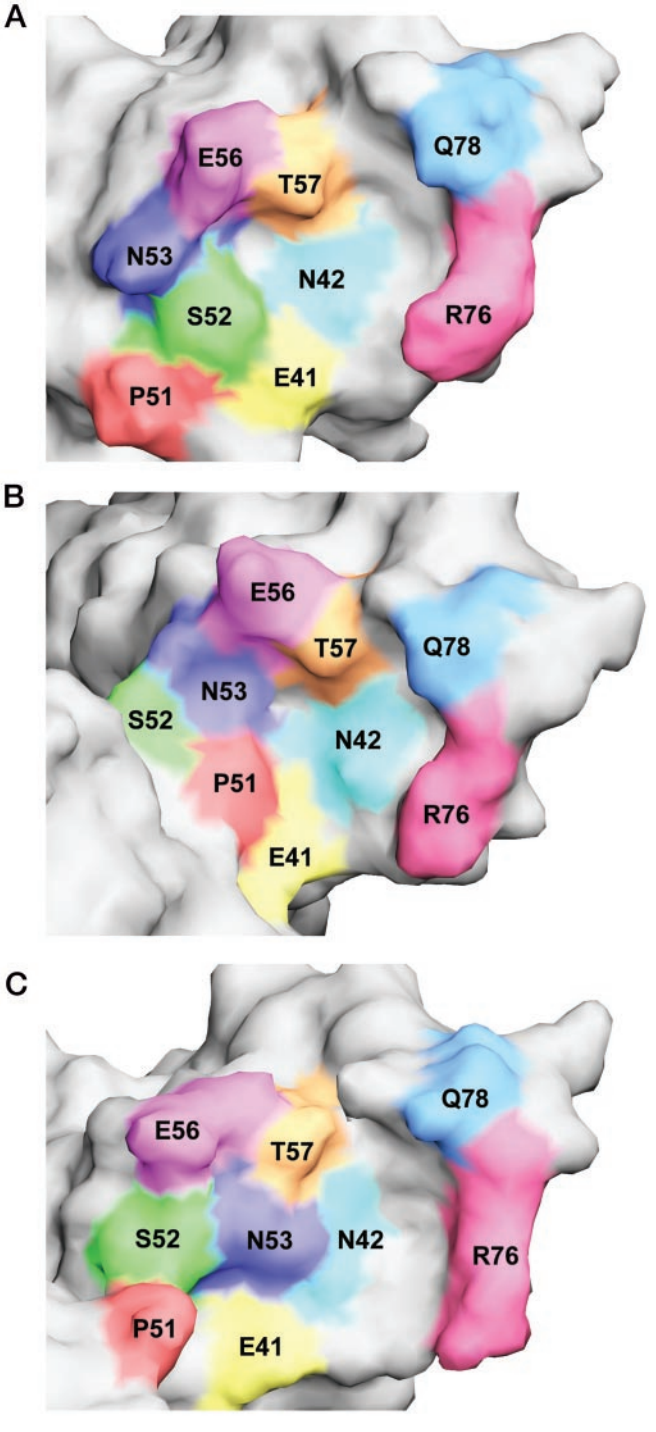

FIG. 3. **Primary oligosaccharide-binding site architectures are shown in the compact monomer (*A*), the low pH domain-swapped structure (*B*), and the high pH domain-swapped structure (*C*).**

TABLE II
Isothermal titration calorimetry results for CHES binding

	ΔH	TΔS	ΔG[a]	K_d	*N* (CHES:CV-N)
	kcal/mol	*kcal/mol*	*kcal/mol*	*mM*	
CHES	0.156 ± 0.009	5.036 ± 0.511	−4.881 ± 0.511	0.3 ± 0.2	1.00

[a] $\Delta G = -RT\ln K_a$; T = 303 K.

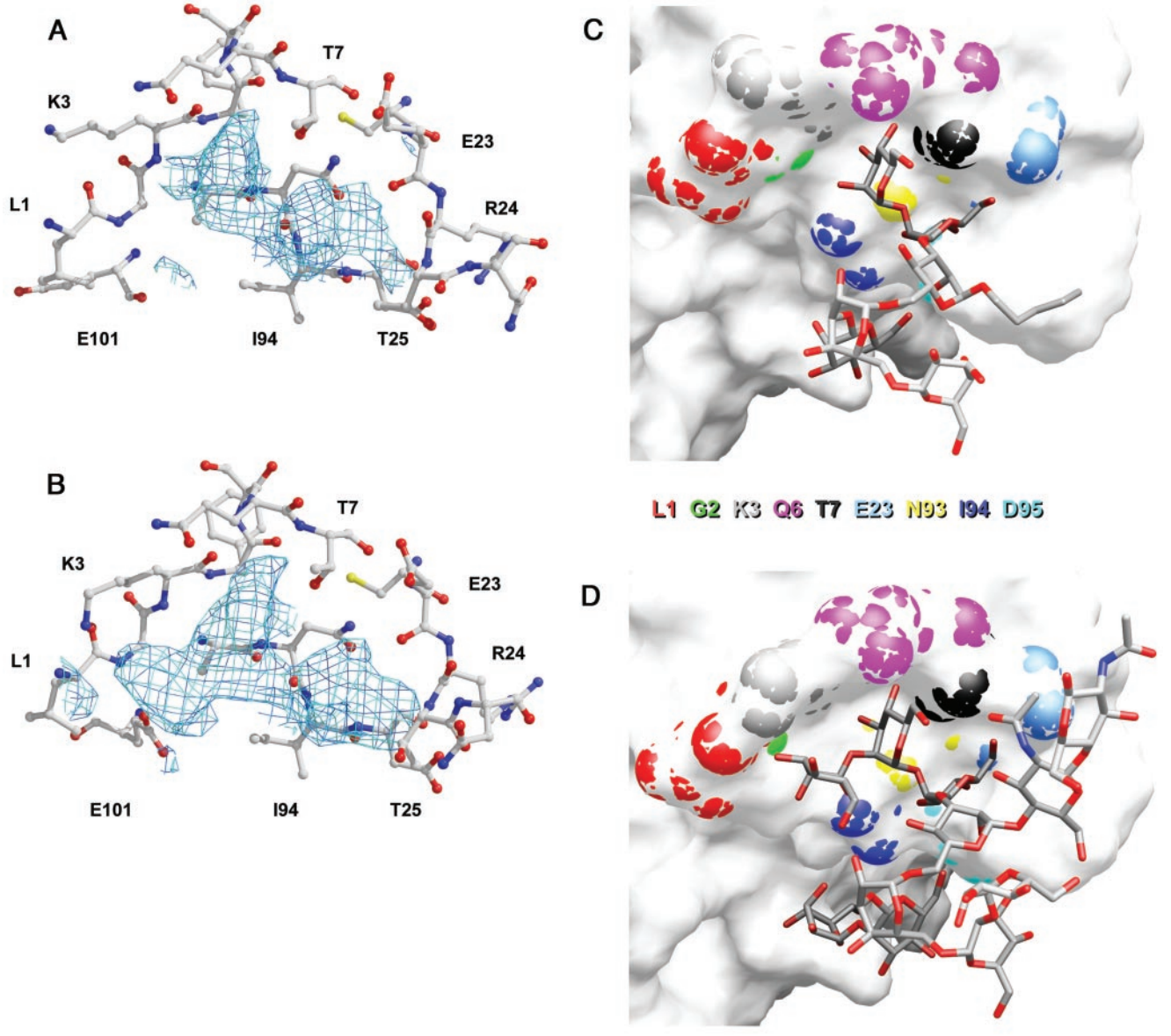

FIG. 4. **Unbiased $F_o - F_c$ difference electron density maps of the binding interfaces contoured at 2.0-σ level and the atomic models of bound oligosaccharides.** *A*, the density for the complex with hexamannoside, visible for two stacked mannose rings: C (residue 505) and 4 (residue 504). *B*, the density for the complex with Man-9, visible for three stacked mannose rings: D1 (residue 506), C (residue 505), and 4 (residue 504). The final atomic coordinates of the oligosaccharides and the protein atoms in contact with them are shown for hexamannoside (*C*) and for Man-9 (*D*). *C* and *D* were generated with the program GRASP (42).

complementarity of oligosaccharide and pocket. Specifically, in the low pH (trigonal) crystal structure (15), the sugar-binding pocket as seen in the compact monomeric structures (Fig. 3*A*) is partially changed. The OG oxygen of Ser-52 is displaced from its optimal position in which it provides a hydrogen bond to an oxygen atom from a mannose ring, disrupting one of the important hydrogen bonds and making sterically unfavorable the binding of any saccharide (Fig. 3*B*). This is the case in all trigonal crystal structures at pH 4.6–8.5, which adopt the same domain orientation and do not show oligosaccharide binding in the primary site. The high pH (tetragonal) crystal structures have a different relative orientation of the domains but still show a perturbed binding pocket. In this case, Asn-53 from the hinge region moves farther into the pocket, reducing its volume (Fig. 3*C*) and introducing unfavorable geometry for the specific binding of a mannose ring. Because of these steric considerations, sugar binding in this pocket may not be favorable and was not observed in any of the tetragonal crystal structures at various pH values. Since we do not observe binding into the primary sugar-binding site, the question arises whether the binding of Man-9 into this pocket is also carried out by three stacked rings, as in the secondary binding site, or by two stacked rings only, as reported previously for the dimannoside (30).

The secondary sugar-binding site is located ~35 Å away from the primary site and is not affected by the geometry of the hinge, presenting the same conformation both in monomeric and domain-swapped dimeric CV-N. Comparing the two structures, the stacked position of the rings is evident from the clear electron density. Three rings are seen in the case of Man-9 (Fig. 4*A*), and two are seen in the case of hexamannoside (Fig. 4*B*). Inspection of the Man-9 structure obtained by molecular dynamics (31) reveals that branches D1 and D3 are more accessible for extended interaction than arm D2. The three terminal rings from both arm D1 and arm D3 were modeled into the electron density and refined. Due to the $\alpha 1 \rightarrow 6$ linkage, the

TABLE III
Oligosaccharide–protein hydrogen bonds

Man-9	Ring name[a]	CV-N	Distance
			Å
504 O3	4	B Asp-95 N	3.2
504 O4	4	A Thr-25 N	2.92
504 O6	4	A Glu-23 OE2	3.2
505 O3	C	A Lys-3 N	3.54
505 O3	C	B Asn-93 N	2.67
505 O4	C	A Thr-7 N	3.52
505 O4	C	A Thr-7 OG1	2.87
506 O3	D1	A Gly-2 N	3.13
506 O3	D1	A Lys-3 NZ	3.16
506 O4	D1	A Lys-3 NZ	3.66
Hexamannoside			
504 O3	4	B Asp-95 N	2.9
504 O4	4	B Asp-95 N	3.03
504 O4	4	B Gly-96 N	3.62
504 O4	4	A Thr-25 N	3.57
504 O6	4	A Glu-23 OE2	3.16
505 O3	C	B Asn-93 N	2.79
505 O3	C	A Lys-3 N	3.4
505 O4	C	A Thr-7 N	3.63
505 O4	C	A Thr-7 OG1	3.09

[a] According to nomenclature from Fig. 1.

TABLE IV
Oligosaccharide torsion angles for α1 → 2 linkages

Linkage between rings	Oligosaccharide	ϕ	ψ
		degrees	*degrees*
C → 4	Man-9	−4.5	22.7
C → 4	hexamannoside	−3.6	10.7
D1 → C	Man-9	−39.4	45.9
2 → 1	dimannoside[a]	−48.8	36.9
2 → 1	methyl-dimannoside[b]	−55.5	14.5

[a] From CV-N/dimannoside solution structure (1iiy.pdb) (30).
[b] From methyl-dimannoside crystal structure (34).

geometry of arm D3 is not compatible with the observed electron density; only mannose rings in an α1→2-linked conformation can fit into the Man-9 electron density map. This observation is in agreement with previous results that show that the oligosaccharides interface with CV-N via a branch containing mainly α1→2-linked rings. The position of mannose rings C and 4 (residues 505 and 504) from arm D1 is very similar to the model suggested from the solution structure of a CV-N disaccharide complex (30). However, the stacked rings interact much more tightly with the protein than suggested by the NMR model, making 10 hydrogen bonds for the Man-9 and 9 hydrogen bonds for the hexamannoside binding interface (Table III). Seven of these hydrogen bonds are conserved between the binding rings 4 and C of the two oligosaccharides, but they are not comparable with the dimannoside hydrogen bonds. Mannose ring 4 of the hexamannoside with five sugar-protein hydrogen-bonds the most tightly. However, the higher number of hydrogen bonds for rings 4 and C of hexamannoside does not provide extra affinity as compared with Man-9. In this respect, the terminal ring D1 (residue 506) of Man-9 must be responsible for the orders of magnitude higher affinity of this ligand. The D1 ring forms three hydrogen bonds with Gly-2 and Lys-3 and could also interact with the flexible Glu-101 from domain B. These important interactions of the terminal ring D1 were not accounted for in a recent mutagenesis study of the secondary sugar-binding site using a two-ring binding interface model (32). The branching mannose ring (residue 503) can also be identified in both maps, suggesting that the α1→2-linked stacked rings are of the main D1 arm. Since the only difference between the D1 branches in Man-9 and hexamannoside is the lack of one α1→2-linked mannose ring (residue 506) at the end of the branch in the latter, the density unequivocally identifies the D1 arm as the binding interface.

The electron density was very clear for the binding interface (residues 504–506) and the branching ring 3 (residue 503) but is less well defined for the rest of the sugar molecule, which is pointing away from the protein. The well defined rings (residues 504–506) were modeled and refined first. These mannopyranose rings adopt the chair conformation with the nonreducing pyranose ring stacked over the reducing mannopyranose. NMR and computational studies show that the conformations of disaccharide fragments of an oligosaccharide fall within the allowed regions of the corresponding disaccharide φ and ψ angle maps (33). If the pyranose rings are treated as flexible during the energy minimization studies of disaccharides, then the φ and ψ conformational space accessed is larger than when the pyranose rings are treated as rigid (33). This seems to be the case of our structures, in which φ and ψ values show more variation, possibly because of the flexibility of the mannopyranose rings. Comparison of the torsion angles for the α1→2 linkages present in the binding interface (Table IV) shows a rather good agreement of the values of φ and ψ for the terminal D1 → C ring linkage in Man-9 with the dimannoside solution structure and the methyl-dimannoside crystal structure (34). The values of φ and ψ are in good agreement for the C → 4 ring linkage in Man-9 and hexamannoside. However, φ shows a 35–50° deviation, and ψ a 5–35° deviation, when compared with the D1 → C linkage in Man-9 and the dimannoside solution structure. Since ring D1 is absent in the hexamannoside, this difference in the torsion angles could be attributed to the steric constraints of the flanking mannopyranoside ring 3 (residue 503) and those of the protein-binding site. The flexible D2 and D3 arms, which point to the solution, can adopt multiple conformations without steric strain on the binding interface. Of the two identical secondary binding sites, one had better electron density. In this site, the bound Man-9 molecule reaches over to a symmetry-related CV-N molecule, contacting residues 15, 59, and 61. These additional interactions might explain the better anchoring of the Man-9 molecule in this site and therefore its better electron density. In the other site, only the D1 arm binding rings and the branching Man-3 were modeled in and refined.

The GlcNAc ring 1 (residue 501) from Man-9 is pointing into the solvent, its most remote atom being located ~14 Å from the CV-N surface. Since this distance was measured in the most extended conformation of Man-9 bound to the secondary binding site, closer positioning of the GlcNAc ring might be possible given the flexibility of the two intermediate rings. GlcNAc 1 is anchored by an Asn residue on the surface of gp120, positioning bound gp120 much closer to CV-N than suggested previously (10). Therefore, besides oligosaccharide-mediated interactions, discrete protein-protein interactions might also play a role in the gp120-CV-N binding (12).

Several co-crystallization conditions were identified for CV-N with hexamannoside. However, the co-crystal structures did not show any sugar binding. This lack of hexamannoside binding to the secondary binding site of CV-N is similar to the results of solution phase NMR experiments in which binding of the hexamannoside to the secondary binding site was not detected (13). Also, soaks with a synthetic nonamannoside and trimannoside did not yield binding in their respective crystal structures. In both synthetic oligosaccharides, a short hydrophobic pentyl segment substituted GlcNAc 1 and 2. Nonamannoside had a tendency to disorder the crystals, raising the mosaicity significantly. The Man-9-CV-N complex structure shows that the branching Man-3 is already protruding from the binding site, interacting partially with the flexible loop region

(residues 22–27). The position of the pentyl is further restricted in nonamannoside by the bulk of the longer branches and might not interact favorably with the flexible loop region, lowering considerably the binding affinity of the sugar and at the same time having a chaotropic effect on the ordered molecules in the crystal.

CV-N undergoes conformational changes upon binding of gp120 and gp41 (6, 9, 35) with an average 11% loss of β-sheet and 2% loss of helical structure. We attempted to determine whether this reflects in the flexibility of the loop in the uncomplexed and sugar-bound forms of CV-N by comparing the B-factors of these structures. There is a well conserved trend of higher than average B-factors in the regions with residues 20–30, 50–57, and 70–80 (data not shown). Not surprisingly, these are residues directly involved in the architecture of sugar-binding sites. This suggests a flexible pocket architecture, which is able to accommodate two or three stacked rings, depending on the structure of the oligosaccharide.

Implications of the Structures for gp120 Binding—The crystallographic data presented here give visual definition to the molecular basis of the unique specificity of CV-N for Man-8 and Man-9 moieties. The additional binding affinity of CV-N for Man-8 and Man-9 as compared with Man-6 or hexamannoside is the result of the additional binding energy derived from the third mannose ring. The physiological significance of this difference is manifested in the relative paucity of Man-8 and Man-9 residues on normal mammalian glycoproteins. Man-8 and Man-9 oligosaccharides are rarely found in the human system and then usually only on glycoproteins destined for short term use and rapid degradation (*e.g.* tissue plasminogen activator). In the case of certain viral glycoproteins, however, Man-8 and Man-9 oligosaccharides are more prevalent. Such is the case of HIV gp120, where as many as 11 high mannose oligosaccharides can be present with five to six of these generally in the form of Man-8 or Man-9 (36). It has been shown that CV-N inhibits the binding of the broadly neutralizing anti-HIV-1 antibody 2G12 (6). Incubation of gp120 with excess CV-N prevents subsequent binding of 2G12 to gp120; however, CV-N binding to gp120 that was preincubated with excess 2G12 was only slightly reduced as compared with binding to gp120 alone (37). These data suggest that 2G12 binds only a subset of the Man1α→2Man termini present on gp120, whereas CV-N binds essentially all such residues (37). The ability of CV-N to target these virus-associated oligosaccharides with high affinity, whereas only binding with relatively low affinity to other, more common, mammalian oligosaccharides (*e.g.* Man-6) is the basis for the potential utility of this agent as an anti-HIV microbicide.

Acknowledgments—We thank L. G. Barrientos and A. M. Gronenborn for helpful discussions.

REFERENCES

1. Piot, P. (1998) *Science* **280,** 1844–1845
2. Burton, D. R. (1997) *Proc. Natl. Acad. Sci. U. S. A.* **94,** 10018–10023
3. Lange, J. M., Karam, M., and Piot, P. (1993) *Lancet* **342,** 1356
4. Boyd, M. R., Gustafson, K. R., McMahon, J. B., Shoemaker, R. H., O'Keefe, B. R., Mori, T., Gulakowski, R. J., Wu, L., Rivera, M. I., Laurencot, C. M., Currens, M. J., Cardellina, J. H., Buckheit, R. W., Jr., Nara, P. L., Pannell, L. K., Sowder, R. C., and Henderson, L. E. (1997) *Antimicrob. Agents Chemother.* **41,** 1521–1530
5. Dey, B., Lerner, D. L., Lusso, P., Boyd, M. R., Elder, J. H., and Berger, E. A. (2000) *J. Virol.* **74,** 4562–4569
6. Esser, M. T., Mori, T., Mondor, I., Sattentau, Q. J., Dey, B., Berger, E. A., Boyd, M. R., and Lifson, J. D. (1999) *J. Virol.* **73,** 4360–4371
7. Geyer, H., Holschbach, C., Hunsmann, G., and Schneider, J. (1988) *J. Biol. Chem.* **263,** 11760–11767
8. Leonard, C. K., Spellman, M. W., Riddle, L., Harris, R. J., Thomas, J. N., and Gregory, T. J. (1990) *J. Biol. Chem.* **265,** 10373–10382
9. O'Keefe, B. R., Shenoy, S. R., Xie, D., Zhang, W., Muschik, J. M., Currens, M. J., Chaiken, I., and Boyd, M. R. (2000) *Mol. Pharmacol.* **58,** 982–992
10. Bewley, C. A., and Otero-Quintero, S. (2001) *J. Am. Chem. Soc.* **123,** 3892–3902
11. Bolmstedt, A. J., O'Keefe, B. R., Shenoy, S. R., McMahon, J. B., and Boyd, M. R. (2001) *Mol. Pharmacol.* **59,** 949–954
12. Shenoy, S. R., O'Keefe, B. R., Bolmstedt, A. J., Cartner, L. K., and Boyd, M. R. (2001) *J. Pharmacol. Exp. Ther.* **297,** 704–710
13. Shenoy, S. R., Barrientos, L. G., Ratner, D. M., O'Keefe, B. R., Seeberger, P. H., Gronenborn, A. M., and Boyd, M. R. (2002) *Chem. Biol.* (*Lond.*), in press
14. Bewley, C. A., Gustafson, K. R., Boyd, M. R., Covell, D. G., Bax, A., Clore, G. M., and Gronenborn, A. M. (1998) *Nat. Struct. Biol.* **5,** 571–578
15. Yang, F., Bewley, C. A., Louis, J. M., Gustafson, K. R., Boyd, M. R., Gronenborn, A. M., Clore, G. M., and Wlodawer, A. (1999) *J. Mol. Biol.* **288,** 403–412
16. Bewley C. A., and Clore, G. M. (2000) *J. Am. Chem. Soc.* **122,** 6009–6016
17. Barrientos, L. G., Campos-Olivas, R., Louis, J. M., Fiser, A., Sali, A., and Gronenborn, A. M. (2001) *J. Biomol. NMR* **19,** 289–290
18. Clore, G. M., and Bewley, C. A. (2002) *J. Magn. Reson.* **154,** 329–335
19. Barrientos, L., Louis, J. M., Botos, I., Mori, T., Han, Z., O'Keefe, B. R., Boyd, M. R., Wlodawer, A., and Gronenborn, A. (2002) *Structure* **10,** 673–686
20. Schlunegger, M. P., Bennett, M. J., and Eisenberg, D. (1997) *Adv. Protein Chem.* **50,** 61–122
21. Gustafson, K. R., Sowder, R. C., Henderson, L. E., Cardellina, J. H., McMahon, J. B., Rajamani, U., Pannell, L. K., and Boyd, M. R. (1997) *Biochem. Biophys. Res. Commun.* **238,** 223–228
22. Botos, I., Mori, T., Cartner, L. K., Boyd, M. R., and Wlodawer, A. (2002) *Biochem. Biophys. Res. Commun.* **294,** 184–190
23. Ratner, D. M., Plante, O. J., and Seeberger, P. H. (2002) *Eur. J. Org. Chem.* **2002,** 826–833
24. Mori, T., Gustafson, K. R., Pannell, L. K., Shoemaker, R. H., Wu, L., McMahon, J. B., and Boyd, M. R. (1998) *Protein Expression Purif.* **12,** 151–158
25. Otwinowski, Z., and Minor, W. (1997) *Methods Enzymol.* **276,** 307–326
26. Navaza, J. (1994) *Acta Crystallogr. Sect. A* **50**, 157–163
27. Brünger, A. T., Adams, P. D., Clore, G. M., DeLano, W. L., Gros, P., Grosse-Kunstleve, R. W., Jiang, J. S., Kuszewski, J., Nilges, M., Pannu, N. S., Read, R. J., Rice, L. M., Simonson, T., and Warren, G. L. (1998) *Acta Crystallogr. Sect. D Biol. Crystallogr.* **54**, 905–921
28. Jones, T. A., and Kieldgaard, M. (1997) *Methods Enzymol.* **277,** 173–208
29. Kleywegt, G. J., and Jones, T. A. (1997) *Methods Enzymol.* **277,** 208–230
30. Bewley, C. A. (2001) *Structure* **9,** 931–940
31. Woods, R. J., Pathiaseril, A., Wormald, M. R., Edge, C. J., and Dwek, R. A. (1998) *Eur. J. Biochem.* **258,** 372–386
32. Chang, L. C., and Bewley, C. A. (2002) *J. Mol. Biol.* **318,** 1–8
33. Rao, V. S. R., Qasba, P. K., Balaji P. V., and Chandrasekaran, R. (1998) *Conformation of Carbohydrates*, Harwood Academic Publishers, Amsterdam, The Netherlands
34. Srikrishnan, T., Chowdhary, M. S., and Matta, K. L. (1989) *Carbohydr. Res.* **186,** 167–175
35. Mariner, J. M., McMahon, J. B., O'Keefe, B. R., Nagashima, K., and Boyd, M. R. (1998) *Biochem. Biophys. Res. Commun.* **248,** 841–845
36. Yeh, J. C., Seals, J. R., Murphy, C. I., van Halbeek, H., and Cummings, R. D. (1993) *Biochemistry* **32,** 11087–11099
37. Scanlan, C. N., Pantophlet, R., Wormald, M. R., Ollmann, S. E., Stanfield, R., Wilson, I. A., Katinger, H., Dwek, R. A., Rudd, P. M., and Burton, D. R. (2002) *J. Virol.* **76,** 7306–7321
38. Brünger, A. T. (1992) *Nature* **355,** 472–474
39. Esnouf, R. M. (1997) *J. Mol. Graph. Model.* **15,** 132–134
40. Meritt, E. A., and Murphy, M. E. P. (1994) *Acta Crystallogr. Sect. D Biol. Crystallogr.* **50**, 869–873
41. Christopher, J. A. (1998) *SPOCK: The Structural Properties Observation and Calculation Kit*, Version 1.06170, The Center for Macromolecular Design, Texas A&M University, College Station, TX
42. Nicholls, A., Sharp, K. A., and Honig, B. (1991) *Proteins Struct. Funct. Genet.* **11,** 281–296